Inorganic Chemistry

Article

pubs.acs.org/IC

Kinetic Analysis of the Formation and Decay of a Non-Heme Ferric Hydroperoxide Species Susceptible to O−O Bond Homolysis

Qiao Zhang and Christian R. Goldsmith*

Department of Chemistry and Biochemistry, Auburn University, Auburn, Alabama 36849, United States

Supporting Information

ABSTRACT: The formation of a ferric hydroperoxide species from $[Fe(bbpc)(MeCN)_2]^{2+}$ (bbpc = *N,N′*-dibenzyl-*N,N′*-bis(2-pyridylmethyl)-1,2-cyclohexanediamine) and its subsequent decomposition were analyzed kinetically. The rate of decay is not strongly influenced by the presence of either water or substrate, suggesting that the ferric hydroperoxide degrades through O−O bond homolysis and is not the relevant metal-based oxidant in the observed catalysis of C−H activation. The rate law corresponding to the complex's formation from O_2 is consistent with the intermediacy of a mononuclear ferric superoxo species.

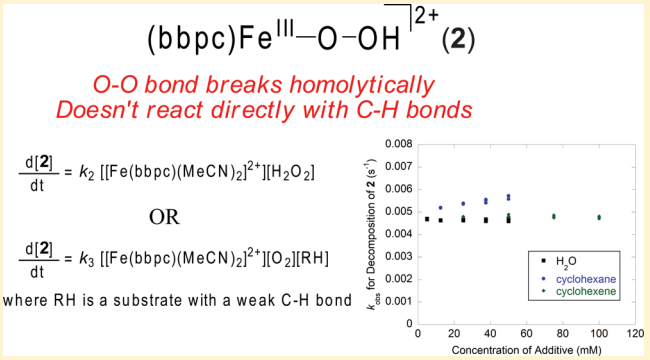

INTRODUCTION

C−H bonds, particularly those on aliphatic carbons, are notoriously difficult to modify chemically. The key difficulty in activating these functional groups is that the harsh oxidants and reaction conditions generally needed for such chemical transformations tend to overoxidize hydrocarbon substrates. This has prompted much research into developing synthetic options that work under milder conditions.[1−3] Among these are processes that rely on nonheme iron catalysts, which have been designed to mimic metalloenzymes capable of catalyzing alkane oxidation under ambient conditions.[4−7] These catalysts are particularly attractive since they rely upon an inexpensive and naturally abundant metal for activity. In these systems, the general consensus is that the terminal oxidant reacts with an iron(II) precursor to convert it to a higher-valent species that is ultimately responsible for C−H activation. Ferric hydroperoxide and ferryl species are commonly proposed as intermediates in this chemistry and have been amply observed in both enzymatic and small-molecule systems.[8−24]

One difficulty has been identifying the metal-based oxidant responsible for C−H activation. Whether ferric hydroperoxide species can directly activate C−H bonds is still debated.[17−19,25,26] Complicating matters is that the O−O bonds of these species can break either homolytically or heterolytically; this may give rise to fundamentally different sorts of reactivity.[12,18] Que has found strong evidence against the direct oxidation of alkene and alkane substrates by low-spin Fe(III)-OOH species susceptible to heterolytic O−O cleavage.[6,12,19] Nam, conversely, has found evidence for the direct involvement of a high-spin Fe(III)-OOH complex that decomposes through homolytic O−O cleavage, although the analysis is complicated by the rapid degradation of the complex to a ferryl oxidant in the absence of substrate.[17,18]

We recently generated an Fe^{III}−OOH species with the ligand *N,N′*-dibenzyl-*N,N′*-bis(2-pyridylmethyl)-1,2-cyclohexanediamine (bbpc; Scheme 1).[8,24] The ferric complex can be

Scheme 1

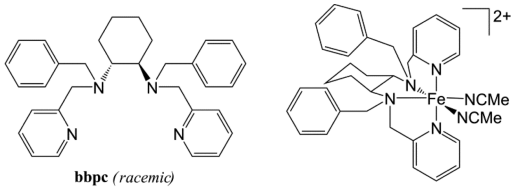

$[Fe(bbpc)(MeCN)_2]^{2+}$ (**1**, *R,R*-diastereomer shown)

prepared from $[Fe(bbpc)(MeCN)_2](SbF_6)_2$ (**1**; Scheme 1) through reactions with either H_2O_2 or O_2. The O_2 reactivity requires a substrate with a weak C−H bond, and the observation of a primary kinetic isotope effect with 9,10-dihydroanthracene (k_H/k_D = 6.8) for the formation of Fe^{III}−OOH suggests that it may be preceded by a ferric superoxide oxidant (Scheme 2).[8] The assignment of the Fe^{III}−OOH intermediate was supported by UV/vis, EPR, and resonance Raman data.[8,24] Although mass spectrometry suggests that the composition of

Scheme 2

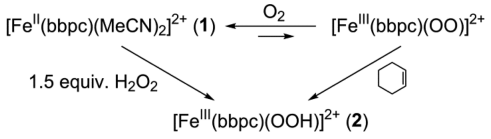

Received: February 17, 2014
Published: May 2, 2014

   dx.doi.org/10.1021/ic5003786 | *Inorg. Chem.* 2014, 53, 5206−5211

the complex is $[Fe(bbpc)(MeCN)(OOH)]^{2+}$,[8] we cannot rule out that a portion of the Fe(III) exists as $[Fe(bbpc)(OOH)]^{2+}$, with the metal center being either penta- or hexacoordinate. Pentacoordination, which would correspond to a terminally bound hydroperoxide ligand, has been observed in the crystal structure of the related $[Fe(bbpc)Cl]^{+}$ (Figure S1, Supporting Information). Strong steric repulsions between the ligands were evident in the metrical parameters of $[Fe(bbpc)Cl_2]$, and similar interactions could potentially spur dissociation of the MeCN from $[Fe(bbpc)(MeCN)(OOH)]^{2+}$.[24] Electron paramagnetic resonance (EPR) spectroscopy suggests that the ferric complex undergoes a spin crossover and is likely high spin at room temperature;[8] regrettably, the complex is not sufficiently stable at room temperature ($t_{1/2} \approx 2$ min) to allow the spectroscopic measurements needed to confirm this assignment. For the sake of simplicity, we refer to the ferric hydroperoxide species as $[Fe(bbpc)(OOH)]^{2+}$ (**2**) throughout this article, with the caveat that this may well be a mixture of closely related ferric hydroperoxide complexes in equilibrium with each other.

Here, we have used stopped-flow kinetics to investigate the formation and decay of **2**. We have determined the influence of several additives, notably acid, water, and hydrocarbon substrates, on the rates of formation and decomposition of the Fe^{III}–OOH species. The results are consistent with the complex decaying through O–O homolysis, rather than heterolysis. Additionally, the presence of substrates that undergo oxidation catalyzed by the ferrous precursor does not impact the rate of decomposition of the ferric hydroperoxide species, suggesting that it is not the relevant oxidant for C–H activation.

EXPERIMENTAL SECTION

Materials. Except where noted otherwise, all chemicals were purchased from Sigma-Aldrich and used as received. Dry dioxygen (O_2) was purchased from Airgas. Anhydrous acetonitrile (MeCN) was purchased from Acros Organics. Hydrogen peroxide (H_2O_2, 50 wt %) was bought from Fisher; its concentration was confirmed to be 50.5 wt % via a titration with $KMnO_4$ and H_2SO_4 in water solution. The ligand *N*,*N*′-dibenzyl-*N*,*N*′-bis(2-pyridylmethyl)-1,2-cyclohexanediamine (bbpc) and its ferrous complex $[Fe(bbpc)(MeCN)_2](SbF_6)_2$ (**1**) were synthesized and identified as described previously.[24]

Instrumentation. A Hi-Tech SF-51 stopped-flow spectrophotometer was used for the described stopped-flow kinetic studies. The reactions were monitored at either 690 or 535 nm with data points taken every 0.2 s. These wavelengths were chosen since they displayed the greatest changes in absorbance during the reactions corresponding to the formation and decay of $[Fe(bbpc)(OOH)]^{2+}$ (**2**). A Hi-Tech C-400 circulator was used to control and maintain the temperature. The program Olis 4300 was used for data acquisition. GraphPad Prism 6 was used for data analysis. A Varian Cary 50 spectrophotometer was used to collect routine optical data; software from the WinUV Analysis Suite was used to process and analyze these data.

Reactivity: Oxidation of 1 by H_2O_2. For each stopped-flow kinetics experiment, 0.20 mL aliquots from two syringes, one filled with **1** in MeCN (**A**) and one filled with H_2O_2 in MeCN (**B**), were simultaneously injected into the instrument. Additives, if present, were introduced via syringe **B**. The solutions were mixed for 1.0 s before the data acquisition began. The spectrophotometer was set to 690 nm, which corresponds to the peak absorbance of a strong ligand to metal charge transfer feature associated with **2**.[24] For most experiments, the initial concentration of **1** after mixing was 0.50 mM. The concentration of **1** was controlled and varied by diluting a 1.0 mM stock solution with pure MeCN. Unless stated otherwise, the initial concentration of H_2O_2 after mixing was 5.0 mM. Except for the variable-temperature experiments, the reactions were run at 298 K.

Reactivity: Oxidation of 1 by O_2. The reactions involving the oxidation of **1** by O_2 proceeded in a manner analogous to those involving H_2O_2. For each experiment, 0.20 mL aliquots from two syringes, one containing an aerobic solution of **1** (**A**) and one containing an aerobic solution of cyclohexene (**B**), were simultaneously injected into the stopped-flow instrument. The solutions were mixed for 1.0 s prior to the start of data acquisition. Additives, if any, were introduced via syringe **B**. The aerobic solutions were prepared by bubbling pure O_2 through anhydrous MeCN for 20 min at room temperature, resulting in stock solutions containing 8.1 mM O_2.[27] The concentration of O_2 was controlled and varied via dilution with solutions made with degassed anhydrous MeCN. The initial concentration of cyclohexene (C_6H_{10}) was 100 mM unless stated otherwise. The stopped-flow spectrometer was set to 535 nm to monitor the changes in absorbance, since intermediate **2** does not form cleanly when generated from O_2 and C_6H_{10}.[8] The previously observed side reactivity prompted us to limit the analysis to an initial rates analysis of the formation of **2**. All reactions involving O_2 as a reagent were run at 298 K.

Data Analysis. All kinetic data were modeled using the GraphPad Prism 6 program. All reactions were repeated at least three times in order to confirm their reproducibility and to assess the precision of the measurements. All first-order or pseudo-first-order processes were allowed to proceed for at least 5 half-lives. All calculated activation parameters were obtained from measurements taken at four temperatures. Data points were taken at each temperature, and the entire experiment was repeated two additional times with fresh stock solutions in order to confirm the reproducibility of the obtained values of $\Delta H^{\ddagger}$ and $\Delta S^{\ddagger}$. Whenever a rate or a rate constant was correlated to the concentration of a reagent, at least four different concentrations of that reagent were investigated. Initial rates were estimated using the 11 data points taken from 1.0 to 3.0 s. In each case, the change in absorbance scaled linearly with time, validating the initial rate approximation.

RESULTS

Generation of $[Fe(bbpc)(OOH)]^{2+}$ from H_2O_2. An Fe^{III}–OOH species (**2**) was previously generated from the reaction between H_2O_2 and $[Fe(bbpc)(MeCN)_2](SbF_6)_2$ (**1**) in acetonitrile (MeCN).[8,24] When the reaction is followed by UV/vis, the changes in absorbance can be fit satisfactorily to an A → B → C model, with species B corresponding to **2**. The concentration of **2** is directly correlated to the intensity at 690 nm.[24] Under normal conditions, the intensity peaks between 20 and 30 s after the reaction begins. The absorbance at 690 nm increases linearly until 4–6 s after the reagents are combined, the exact time being dependent upon the reaction conditions. The linearity suggested that an initial rate analysis of these data would be feasible. Consequently, we varied the starting concentrations of the reagents and measured the changes in absorbance at 690 nm from 1 to 3 s to get an approximation of the initial rates. Prior to 1 s, the data were noisy, likely due to lingering turbulence from the mixing with our particular instrument and set-up; this necessitated the truncation of the data.

The first two series of experiments were run in MeCN at 298 K. The initial concentration of **1** was varied between 0.10 and 0.80 mM with a set 5.0 mM initial concentration of H_2O_2. Subsequently, the concentration of H_2O_2 was varied from 0.50 to 5.0 mM with a set initial concentration of 0.50 mM **1**. In both series, the changes in absorbance from 1 to 3 s scale linearly with higher concentrations of the investigated reagent, indicating that the formation of **2** is first order with respect to both **1** and H_2O_2. Under such conditions, the formation of **2** follows the rate law described by eq 1.

The formation of **2** from 0.50 mM **1** and 5.0 mM H_2O_2 was studied in MeCN from 294 to 324 K. The temperature-dependent

dx.doi.org/10.1021/ic5003786 | Inorg. Chem. 2014, 53, 5206–5211

$$d[\mathbf{2}]/dt = k_2[\mathbf{1}][H_2O_2] \quad (1)$$

second-order rate constants for the formation of **2** were calculated from values of k_{obs} obtained from the fits of the A → B → C model to the data. Subsequently, these were used to prepare an Eyring plot (Figure 1). $\Delta H^{\ddagger}$ and $\Delta S^{\ddagger}$ were

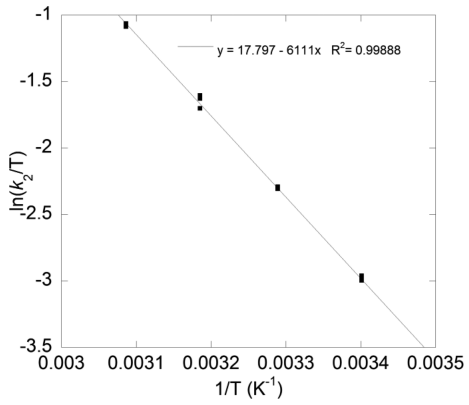

Figure 1. Eyring plot for the formation of **2** from a reaction between 0.50 mM **1** and 5.0 mM H_2O_2 in MeCN at temperatures ranging from 294 to 324 K. The reactions were followed using the absorbance at 690 nm. All of the second-order rate constants from three independent sets of experiments are plotted. The calculated $\Delta H^{\ddagger}$ value was 50.5 (±0.5) kJ mol^{-1}. The calculated $\Delta S^{\ddagger}$ value was −50 (±2) J K^{-1} mol^{-1}.

calculated to be 50.5(±0.5) kJ mol^{-1} and −50(±2) J mol^{-1} K^{-1}, respectively. The negative entropy of activation is consistent with an associative process, corroborating the bimolecular rate law suggested by the initial rate analysis (eq 1).

Various concentrations of H_2O and two oxidizable substrates, cyclohexane (C_6H_{12}) and cyclohexene (C_6H_{10}), were added, but none of these additives influenced the rate of formation of **2** from **1** and H_2O_2 to a significant degree (Figure 2). Water

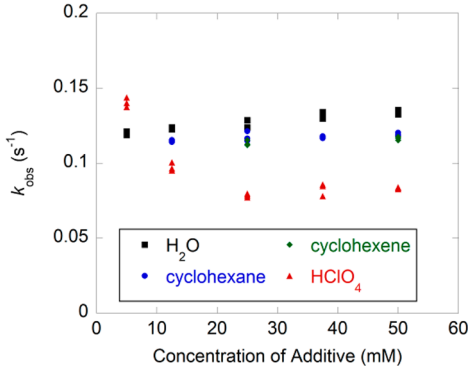

Figure 2. Influence of additives on the k_{obs} value for the formation of **2** from 0.50 mM **1** and 5.0 mM H_2O_2 in MeCN at 298 K. The data from three independent series of experiments are plotted for each additive.

might have been expected to inhibit the formation of **2** by acting as a competing ligand, but the data instead suggest that H_2O cannot compete effectively with H_2O_2 for binding sites on the iron. Conversely, the k_{obs} value for the formation of **2** from 0.50 mM **1** and 5.0 mM H_2O_2 increases slightly (~10%) as the concentration of water increases from 5.0 to 50 mM (Figure 2). Aliquots of $HClO_4$ were also added to determine if the presence of an acid influenced the rate of formation. A noticeable decrease in the k_{obs} value is observed when over 5 equiv of $HClO_4$ (2.5 mM) are added. The addition of $NaClO_4$ had a similar, but smaller, effect. The k_{obs} value for the formation of **2** from **1** and 5.0 mM H_2O_2 was 0.095 s^{-1} in the presence of 50 mM $NaClO_4$ and 0.083 s^{-1} in the presence of $HClO_4$.

Decomposition of [Fe(bbpc)(OOH)]$^{2+}$. The decomposition of **2** formed from H_2O_2 and **1** can be followed by the loss of the 690 nm UV/vis band associated with **2** and fit to a simple B → C step. When the initial concentration of H_2O_2 was varied, it was found that excess terminal oxidant hastens the disappearance of **2**, as confirmed from the higher k_{obs} value for the B → C step from the fits to the data. Similar observations have been made in other mononuclear non-heme iron systems and have been used to explain the lessened oxidative efficiency for hydrocarbon oxidation catalysis with higher loadings of terminal oxidant.[28] At higher concentrations of H_2O_2, the relationship between $[H_2O_2]$ and the observed rate constant for the decay appears to be linear, suggesting that H_2O_2 is reacting directly with **2**. The large y intercept would suggest other pathways for decomposition that are independent of $[H_2O_2]$.

The addition of C_6H_{12}, which is oxidized to cyclohexanol and cyclohexanone under these conditions,[24] fails to significantly alter the rate of decomposition of **2** (Figure 3). A 10% increase

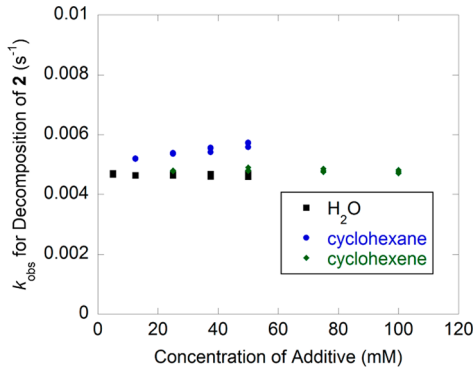

Figure 3. Influence of additives on the k_{obs} value for the decomposition of **2** formed from 0.50 mM **1** and 5.0 mM H_2O_2 in MeCN at 298 K. The data from three independent sets of experiments are plotted for each additive. The k_{obs} value for the decomposition of **2** by itself was found to be 0.0044 s^{-1}.

in the rate of decay is observed as the concentration of C_6H_{12} is increased from 5.0 to 50 mM, but this is unlikely to result from a direct reaction between **2** and C_6H_{12}. The addition of C_6H_{10}, which has more readily oxidized allylic C−H bonds, would be anticipated to increase k_{obs} if substrate oxidation were involved in the rate-determining step (RDS). This substrate, however, likewise fails to increase the rate of the disappearance of **2** relative to the substrate-free baseline, even at concentrations as high as 100 mM (Figure 3).

It had been previously observed that H_2O hastens the disappearance of some, but not all, ferric hydroperoxide species.[10,12] The differences were attributed to water's ability to act as an acid and hasten heterolytic cleavage of the O−O bond. The Fe^{III}−OOH species that were not water-sensitive were proposed to decay instead through homolytic cleavage of the O−O bond. The presence of additional H_2O beyond that added with the H_2O_2 fails to accelerate the rate of decomposition of **2**, even when 100 equiv of H_2O relative to iron is present (50 mM, Figure 3).

dx.doi.org/10.1021/ic5003786 | Inorg. Chem. 2014, 53, 5206−5211

The O−O bond likely cleaves in the RDS of the decomposition reaction. The temperature dependence of the k_{obs} value from the decay portion of the reaction between 0.50 mM **1** and 5.0 mM H_2O_2 was assessed from 294 to 324 K. An Eyring plot prepared from these data yields the following kinetic parameters: $\Delta H^{\ddagger}$ = 53.2(±1.1) kJ mol^{-1} and $\Delta S^{\ddagger}$ = −68(±4) J mol^{-1} K^{-1} (Figure 4).

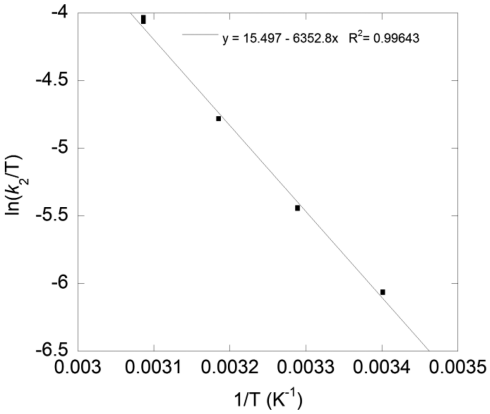

Figure 4. Eyring plot for the decomposition of **2** formed from a reaction between 0.50 mM **1** and 5.0 mM H_2O_2 in MeCN at temperatures ranging from 294 to 324 K. The reactions were followed using the absorbance at 690 nm. The data from three independent experiments are plotted. The calculated $\Delta H^{\ddagger}$ value was 53.2(±1.1) kJ mol^{-1}. The calculated $\Delta S^{\ddagger}$ value was −68(±4) J K^{-1} mol^{-1}.

Generation of [Fe(bbpc)(OOH)]$^{2+}$ from O_2. In studies using 1,4,8,11-tetramethyl-1,4,8,11-tetraazacyclotetradecane (TMC) as a ligand, Nam and co-workers had observed the formation of ferryl species, prompting them to posit that the initially generated oxidant was a ferric superoxo species.[9] Subsequent work from ourselves with the bbpc ligand had found that the rate of formation of **2** was first order with respect to the concentration of C_6H_{10} or an analogous allylic or benzylic substrate; the rate of formation also slowed when a deuterated substrate was used.[8] On the basis of these observations plus the detection of organic radicals in these reaction mixtures, we proposed that the formation of **2** proceeds through a ferric superoxo species, which abstracts a hydrogen atom from the hydrocarbon to yield **2** and an organic radical.

The formation of **2** from mixtures of **1**, O_2, and cyclohexene was further investigated, with an interest in determining the reaction's dependence on O_2 and **1**. A kinetic analysis was performed, with the changes in absorbance at 535 nm from 1 to 3 s serving as approximations of the initial rates. The 690 nm feature does not develop strongly enough in most of these reactions to serve as a reliable spectroscopic tag for the concentration of **2**, necessitating that we instead monitor the reactions at 535 nm.[8] As the concentration of O_2 was increased with set concentrations of cyclohexene and **1**, the changes in the absorbance from 1 to 3 s are most consistent with a first-order dependence on [O_2]. The changes in absorbance from 1 to 3 s likewise scale linearly with the initial concentration of **1**. The rate law can be described by eq 2.

$$d[\mathbf{2}]/dt = k_3[\mathbf{1}][O_2][C_6H_{10}] \quad (2)$$

DISCUSSION

Prior studies of ferric hydroperoxide species have found that their formation from ferrous precursors and H_2O_2 occurs in two steps: (1) the first $^1/_2$ equiv of H_2O_2 oxidizes 1 equiv of Fe(II) to Fe(III), and (2) the remaining H_2O_2 substitutes for one of the ligands on the initially generated ferric product to yield an Fe^{III}−OOH complex.[23] The initial rate analysis of the formation of [Fe(bbpc)(OOH)]$^{2+}$ (**2**) from [Fe(bbpc)(MeCN)$_2$]$^{2+}$ (**1**) and H_2O_2 suggests that, at higher concentrations of the reagents, the rate-determining step (RDS) involves a bimolecular collision between **1** and H_2O_2. This conclusion is supported by the highly negative $\Delta S^{\ddagger}$ value obtained from kinetic data acquired over several temperatures (Figure 1). Although the reaction stoichiometry suggests that 1 equiv of H_2O_2 will lead to the one-electron oxidation of two Fe(II) centers, the rate law determined by the initial rate analysis suggests that the RDS involves only 1 equiv of Fe(II). This would be inconsistent with formation of a diiron peroxide-bridged species, which may be conceived as the simplest means to oxidize two iron centers with one molecule of H_2O_2. The data at low concentrations of **1**, however, deviate from the linear relationship established at higher concentrations. One possible explanation for this deviation is that a subsequent reaction between the 1:1 iron−H_2O_2 adduct and another 1 equiv of iron may become the RDS under such conditions.

The influences of various additives on the rates of formation and decay were assessed. These included two substrates that are readily oxidized by mixtures of **1** and H_2O_2: cyclohexane and cyclohexene.[8,24] The results suggest that H_2O does not have a major role in the oxidation of the iron (Figure 2). Indeed, the only tested additives that influenced the formation of **2** were $HClO_4$ and $NaClO_4$, which both slowed the rate of formation of **2** from **1** and H_2O_2. Excess H_2O_2 appears to promote the more rapid degradation of **2** (Figure 3). Although H_2O_2 could potentially be a substrate, with O−H bond dissociation energies of approximately 88 kcal mol^{-1},[29] the inability of cyclohexane (C_6H_{12}) or cyclohexene (C_6H_{10}) to hasten the decomposition of **2** may suggest that the excess H_2O_2 reacts with **2** by other means, perhaps through the formation of a more reactive species.

None of the other additives, including the two hydrocarbon substrates, affect the rate of decomposition of **2** (Figure 3). The data therefore suggest that **2** is not directly responsible for the catalyzed C−H activation and that the hydrocarbon oxidation instead occurs during a step subsequent to the RDS of the Fe^{III}−OOH compound's decay. This contrasts with recent results from Nam's group, who found that the lifetime of a high-spin Fe^{III}−OOH complex generated with the TMC ligand decreases as the concentration of an added hydrocarbon substrate increases.[17] The addition of H_2O or acid likewise fails to accelerate the disappearance of **2**; this is consistent with a decay process involving homolysis, rather than heterolysis, of the O−O bond.[10,12] Nam's Fe^{III}−OOH complex likewise decomposes through O−O homolysis.[17]

Additional, albeit weaker, support for homolytic cleavage is provided by the kinetic parameters (Figure 4). The $\Delta H^{\ddagger}$ value for the decay of **2** is more similar to those of non-heme Fe^{III}−OOH species that undergo homolytic O−O cleavage than to those that react through O−O heterolysis.[12,17,18] Although the $\Delta S^{\ddagger}$ value for the decomposition of **2** falls comfortably within the range previously observed for nonheme Fe^{III}−OOH species, these values do not distinguish homolytic from heterolytic O−O cleavage.[12] The negative $\Delta S^{\ddagger}$ is curious, since **2**

dx.doi.org/10.1021/ic5003786 | Inorg. Chem. 2014, 53, 5206−5211

presumably degrades through a unimolecular reaction. Groves and Watanabe had invoked the coordination of an additional ligand to the iron in the transition state to explain the negative entropies of activation calculated for the O−O bond cleavage associated with heme peroxo complexes.[30,31] We currently have no data, however, that would corroborate this in our own system.

Prior results from our laboratory found that O atom exchange appears to occur between **2** and H_2O, suggesting that the cleavage of the O−O bond is reversible.[8] The reversibility of the O−O cleavage may indicate that the hydroxyl radical generated from homolytic cleavage of the OOH ligand remains associated with the iron-containing product, which is isoelectronic with a ferryl species (Scheme 3). Whether the two

Scheme 3

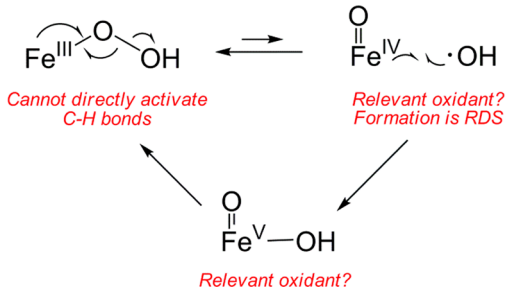

combine into an Fe(V) species prior to re-formation of the O−O bond remains unclear, and we cannot preclude it as a possibility at this time. The close association of the hydroxyl radical with the ferryl species would be a possible explanation for the observed regioselectivity of the alkane oxidation catalyzed by **1**, which shows a stronger than usual preference for oxidizing C−H bonds on secondary carbons over those on tertiary carbons.[24] The regioselectivity is inconsistent with the agency of freely diffusing hydroxyl radicals.[6]

Reversible O−O cleavage may also explain the discrepancy between our results and those of Nam's research group. A rapid interconversion between ferric species and higher-valent oxidants would render the Fe^{III}−OOH susceptible to reactions with oxidizable C−H bonds, at rates approaching those of the Fe^{IV}=O oxidant. An unidentified equilibrium between these two may explain the previously noted similarities in the rates of hydrocarbon oxidation reactions involving Fe^{III}−OOH and Fe^{IV}=O complexes with TMC.[17,18]

The Fe^{III}−OOH species can also be generated from reactions between **1**, O_2, and substrates with weak C−H bonds.[8] Prior work from our laboratory found that the rate of the ferric intermediate's formation scales with the concentration of the hydrocarbon substrate. The observation of a primary kinetic isotope effect with 9,10-dihydroanthracene (k_H/k_D = 6.8) suggested that the hydrocarbon serves as a hydrogen atom donor, possibly indicating a ferric superoxo species as an initially generated oxidant. The formation of **2** from O_2 was probed further, with an interest in determining the nuclearity of the immediate precursor to **2**. The rate law suggests that the oxidation of **1** by O_2, with concomitant oxidation of C_6H_{10}, proceeds through a mononuclear, rather than binuclear, iron species; otherwise, the rate law would be second order in iron. The rate law is consistent with our previously hypothesized mechanism, in which a ferric superoxide species abstracts a hydrogen atom from an allylic substrate in the RDS to yield **2** (Scheme 2).[8]

CONCLUSIONS

We have determined that the Fe^{III}−OOH species with the bbpc ligand decomposes through homolysis of the O−O bond. The ferric hydroperoxide species itself does not appear to be the relevant oxidant for C−H activation. The previously observed regioselectivity of the alkane oxidation and the reversibility of the O−O cleavage are inconsistent with freely diffusing radicals, suggesting that any generated hydroxyl radicals remain associated with the higher-valent iron byproduct. We have also determined the rate law associated with the formation of **2** from O_2; this rate law is consistent with the previously proposed intermediacy of a mononuclear ferric superoxo species.

ASSOCIATED CONTENT

Supporting Information

Text, figures, tables, and a CIF file giving crystal structure data for [Fe(bbpc)Cl](SbF_6), initial rate analyses of the formation of **2** from **1**, O_2, and H_2O_2, and the peak absorbance at 690 nm as a function of added $HClO_4$. This material is available free of charge via the Internet at http://pubs.acs.org.

AUTHOR INFORMATION

Corresponding Author

*E-mail for C.R.G.: crgoldsmith@auburn.edu.

Notes

The authors declare no competing financial interest.

ACKNOWLEDGMENTS

The authors thank Auburn University and the American Chemical Society Petroleum Research Fund (Grant #49532-DNI3) for financial support and Prof. David M. Stanbury and his research group for their assistance with the stopped-flow experiments and a presubmission review of this manuscript. The crystal structure of [Fe(bbpc)Cl](SbF_6) in the Supporting Information was solved by Prof. John D. Gorden from a crystal grown by Mr. Christopher F. Cain.

REFERENCES

(1) Gunay, A.; Theopold, K. H. *Chem. Rev.* **2010**, *110*, 1060−1081.
(2) Brückl, T.; Baxter, R. D.; Ishihara, Y.; Baran, P. S. *Acc. Chem. Res.* **2012**, *45*, 826−839.
(3) Shilov, A. E.; Shul'pin, G. B. *Chem. Rev.* **1997**, *97*, 2879−2932.
(4) Costas, M.; Mehn, M. P.; Jensen, M. P.; Que, L., Jr. *Chem. Rev.* **2004**, *104*, 939−986.
(5) Que, L., Jr.; Ho, R. Y. N. *Chem. Rev.* **1996**, *96*, 2607−2624.
(6) Chen, K.; Que, L., Jr. *J. Am. Chem. Soc.* **2001**, *123*, 6327−6337.
(7) Nam, W. *Acc. Chem. Res.* **2007**, *40*, 522−531.
(8) He, Y.; Goldsmith, C. R. *Chem. Commun.* **2012**, *48*, 10532−10534.
(9) Lee, Y.-M.; Hong, S.; Morimoto, Y.; Shin, W.; Fukuzumi, S.; Nam, W. *J. Am. Chem. Soc.* **2010**, *132*, 10668−10670.
(10) Li, F.; Meier, K. K.; Cranswick, M. A.; Chakrabarti, M.; Van Heuvelen, K. M.; Münck, E.; Que, L., Jr. *J. Am. Chem. Soc.* **2011**, *133*, 7256−7259.
(11) Nam, E.; Alokolaro, P. E.; Swartz, R. D.; Gleaves, M. C.; Pikul, J.; Kovacs, J. A. *Inorg. Chem.* **2011**, *50*, 1592−1602.
(12) Oloo, W. N.; Fielding, A. J.; Que, L., Jr. *J. Am. Chem. Soc.* **2013**, *135*, 6438−6441.
(13) Rohde, J.-U.; In, J.-H.; Lim, M. H.; Brennessel, W. W.; Bukowski, M. R.; Stubna, A.; Münck, E.; Nam, W.; Que, L., Jr. *Science* **2003**, *299*, 1037−1039.
(14) Wada, A.; Ogo, S.; Nagatomo, S.; Kitagawa, T.; Watanabe, Y.; Jitsukawa, K.; Masuda, H. *Inorg. Chem.* **2002**, *41*, 616−618.

dx.doi.org/10.1021/ic5003786 | *Inorg. Chem.* 2014, 53, 5206−5211

(15) Ho, R. Y. N.; Roelfes, G.; Hermant, R.; Hage, R.; Feringa, B. L.; Que, L., Jr. *Chem. Commun.* **1999**, 2161−2162.
(16) Martinho, M.; Blain, G.; Banse, F. *Dalton Trans.* **2010**, *39*, 1630−1634.
(17) Cho, J.; Jeon, S.; Wilson, S. A.; Liu, L. V.; Kang, E. A.; Braymer, J. J.; Lim, M. H.; Hedman, B.; Hodgson, K. O.; Valentine, J. S.; Solomon, E. I.; Nam, W. *Nature* **2011**, *478*, 502−505.
(18) Liu, L. V.; Hong, S.; Cho, J.; Nam, W.; Solomon, E. I. *J. Am. Chem. Soc.* **2013**, *135*, 3286−3299.
(19) Park, M. J.; Lee, J.; Suh, Y.; Kim, J.; Nam, W. *J. Am. Chem. Soc.* **2006**, *128*, 2630−2634.
(20) Price, J. C.; Barr, E. W.; Glass, T. E.; Krebs, C.; Bollinger, J. M., Jr. *J. Am. Chem. Soc.* **2003**, *125*, 13008−13009.
(21) Krebs, C.; Fujimori, D. G.; Walsh, C. T.; Bollinger, J. M., Jr. *Acc. Chem. Res.* **2007**, *40*, 484−492.
(22) Galonić, D. P.; Barr, E. W.; Walsh, C. T.; Bollinger, J. M., Jr.; Krebs, C. *Nat. Chem. Biol.* **2007**, *3*, 113−116.
(23) Roelfes, G.; Lubben, M.; Chen, K.; Ho, R. Y. N.; Meetsma, A.; Genseberger, S.; Hermant, R. M.; Hage, R.; Mandal, S. K.; Young, V. G., Jr.; Zang, Y.; Kooijman, H.; Spek, A. L.; Que, L., Jr.; Feringa, B. L. *Inorg. Chem.* **1999**, *38*, 1929−1936.
(24) He, Y.; Gorden, J. D.; Goldsmith, C. R. *Inorg. Chem.* **2011**, *50*, 12651−12660; *Inorg. Chem.* **2012**, *51*, 7431 (correction).
(25) Chen, K.; Costas, M.; Kim, J.; Tipton, A. K.; Que, L., Jr. *J. Am. Chem. Soc.* **2002**, *124*, 3026−3035.
(26) Decker, A.; Chow, M. S.; Kemsley, J. N.; Lehnert, N.; Solomon, E. I. *J. Am. Chem. Soc.* **2006**, *128*, 4719−4733.
(27) Sawyer, D. T.; Chiericato, G., Jr.; Angelis, C. T.; Nanni, E. J., Jr.; Tsuchiya, T. *Anal. Chem.* **1982**, *54*, 1720−1724.
(28) Britovsek, G. J. P.; England, J.; White, A. J. P. *Inorg. Chem.* **2005**, *44*, 8125−8134.
(29) Litorja, M.; Ruscic, B. *J. Electron Spectrosc.* **1998**, *97*, 131−146.
(30) Groves, J. T.; Watanabe, Y. *J. Am. Chem. Soc.* **1986**, *108*, 7834−7836.
(31) Groves, J. T.; Watanabe, Y. *J. Am. Chem. Soc.* **1988**, *110*, 8443−8452.

dx.doi.org/10.1021/ic5003786 | *Inorg. Chem.* 2014, 53, 5206−5211